Journal of Non-Crystalline Solids xxx (xxxx) xxx–xxx

Contents lists available at ScienceDirect

Journal of Non-Crystalline Solids

journal homepage: www.elsevier.com/locate/jnoncrysol

Power-law scaling behaviors for shear band intersections in $Zr_{64.13}Cu_{15.75}Ni_{10.12}Al_{10}$ bulk metallic glass

Bo Shi[a,*], Yuanli Xu[b], Fuan Wei[a], Shiyu Luan[a], Peipeng Jin[a,*]

[a] Qinghai Provincial Key Laboratory of New Light Alloys, Qinghai Provincial Engineering Research Center of High Performance Light Metal Alloys and Forming, Qinghai University, Xining 810016, China

[b] Institute of Materials Science and Engineering, Lanzhou University, Lanzhou 730000, China

ARTICLE INFO

Keywords:
Bulk metallic glass
Compressive deformation
Shear band intersection
Power-law

ABSTRACT

At the large compressive deformation levels, shear band offsets at intersection sites and the stress drop magnitudes of serrated flow follow power-law distributions for $Zr_{64.13}Cu_{15.75}Ni_{10.12}Al_{10}$ bulk metallic glass. In addition, it was revealed that shear band interactions evolve into a process of large degree cooperation of many shear bands via investigating the relation between shear band intersections and serrated flow. To clarify the evolution rules of shear band intersections, quantitatively statistical works were performed. With increasing the plastic strain, the distribution of shear band orientations becomes wider and displays a multi-peak distribution. The average shear band spacing varies as a power function of plastic strain and decreases to a very low level in large deformation stages. Small spacing and arbitrary orientations of shear bands greatly enhance the intersecting probability and lead to the density of shear band intersections varying as a power function of plastic strain. Enormous amount of undeformed regions enclosed by shear bands provide many places for shear bands intersecting.

1. Introduction

At low temperatures and high strain rates, the plastic deformation of metallic glasses is highly localized into shear bands [1]. Because of work softening, a single shear band usually propagates rapidly and results in catastrophic failure. Hence, the macroscopic plasticity of metallic glasses is very low [2]. Some constrained loading conditions can make metallic glasses undergo significant plastic deformation via the formation of multiple shear bands [3,4]. In the aspect of plastic deformation mechanism, with the number of shear bands increasing during plastic deformation, the intersections of shear band will play a more remarkable role, especially in the large deformation stage [5]. Besides, in the aspect of mechanical properties, enhancing the shear band numbers can increase the plasticity [6], and further lead to the number of intersections increasing. It is found that the mechanical performances of metallic glasses are strongly correlated to shear band intersections. For example, strong shear band intersections can lead to geometric hardening behaviors in $Cu_{47.5}Zr_{47.5}Al_5$, $Zr_{64.13}Cu_{15.75}Ni_{10.12}Al_{10}$ and $Pd_{77.5}Cu_6Si_{16.5}$ bulk metallic glasses (BMGs) [7–10]. Thus, it is much more significant to investigate the evolution of shear band intersections. It may also provide some insights for understanding the plastic deformation mechanism and toughening BMGs.

The variation of the number of shear band intersections with plastic strain has been studied previously. The rapid increase of shear band intersections induced hardening, after counteracting free volume induced softening, may lead to an increase in hardness [11]. The density of shear band intersections and the shear band offsets at intersection sites can reflect the degree of interactions between shear bands. However, the evolution laws of them have not been directly and quantitatively studied so far. In addition, theoretical calculations indicate that strong shear band interactions have great influences on serrated flow behaviors [12,13]. For ductile BMGs, stress drop magnitudes of serrations in strain-stress curve follow power-law distribution, which can be attributed to strong shear band interactions. However, in different deformation stages, the relation between shear band intersections and serrated flows remains to be clarified by further experiments.

In the present work, $Zr_{64.13}Cu_{15.75}Ni_{10.12}Al_{10}$ BMG was compressed to different plastic strains. The evolutions of shear band spacing, shear band orientations, and shear band offsets at intersection sites have been quantitatively studied. The average shear band spacing and the density of shear band intersections vary as power functions of plastic strain. In the large deformation stage, shear band orientations display a multiple-peak distribution, shear band offsets and serrated flows follow power-

* Corresponding authors.
E-mail addresses: shibo05@126.com (B. Shi), peipeng.jin@hotmail.com (P. Jin).

http://dx.doi.org/10.1016/j.jnoncrysol.2017.07.005
Received 8 May 2017; Received in revised form 28 June 2017; Accepted 4 July 2017

law distributions.

2. Experimental procedure

Master alloy ingots with nominal composition of $Zr_{64.13}Cu_{15.75}Ni_{10.12}Al_{10}$ were prepared by arc-melting the mixtures of highly pure Zr (99.8%), Cu (99.99%), Ni (99.99%), and Al (99.99%) in a Ti-gettered argon atmosphere. Each ingot was remelted more than six times to ensure chemical homogeneity. BMG rods with a square cross section of $2 \times 2\,mm^2$ were prepared by arc-melting master alloy ingot and subsequent suction-casting into a water-cooled copper mold. The compression test specimens were cut from the as-cast rod. Before compression test, both ends of these specimens were polished to be parallel. The compression tests were performed on a Shijin WDW-100D universal testing machine. In all compression tests, strain rate and aspect ratio are $1 \times 10^{-3}\,s^{-1}$ and 1, respectively. The plastic strain ε_p was denoted as $\varepsilon_p = (h_0 - h) / h_0$, where h_0 is the original height, and h is the height after deformation. The shear band patterns were analyzed by scanning electron microscopy (SEM) using a Hitachi S-4800 field emission scanning electron microscope operating at an acceleration voltage of 5 kV.

The shear band spacing was determined by the following steps: (i) SEM images were taken from thirty random regions for each sample. (ii) A line paralleled to the loading axis was drawn on each SEM image, and this line intersected with shear bands. (iii) The distance between two adjacent crosspoints of this line and shear bands is considered as the shear band spacing. (iv) The total line length was divided by the total number of crosspoints, and this obtained result is regarded as the average shear band spacing. The density of shear band intersections was determined by the following steps: (i) The number of shear band intersections in ten observation regions (each region has an equal area of 113 μm^2) for one sample were counted. (ii) The plane density of intersections for each region was calculated. (iii) The density of shear band intersections is a mean value of all densities for each observation regions. The orientation angle (φ, the angle between an observed shear band line on side surface and horizontal line, ranging from -90° to 90°) distribution was obtained by the following steps: (i) A line paralleled to the loading axis was drawn on each SEM image (ten images were counted for each sample). (ii) Orientation angles of shear bands located on the line were measured. (iii) The frequency of orientation angles who fall into the interval of $(\varphi - \delta\varphi / 2,\ \varphi + \delta\varphi / 2)$ was counted, and the distribution histogram of orientation angles ranging from -90° to 90° was plotted.

3. Results and discussion

To investigate the shear band evolution with plastic strain, the SEM observations and statistical works were performed. The representative SEM images of shear bands for deformed $Zr_{64.13}Cu_{15.75}Ni_{10.12}Al_{10}$ BMG samples with plastic strains of 6% and 83% are shown in Fig. 1, respectively. Only a few shear bands formed in the deformed sample with a plastic strain of 6% (Fig. 1a). The angle between the observed shear band and loading axis is about 47°. Obviously, in small deformation stages, shear bands are separate and free, and the shear band intersections are very few. For the sample with a plastic strain of 83% (Fig. 1b), a large number of fine shear bands form and their orientations are widely distributed. These shear bands form a homogeneous network pattern. Uniformly distributed shear band intersections were observed, indicating severe interactions between shear bands. Shear bands with intersections divide the deformed BMG into two components: one is shear bands, and the other is undeformed amorphous regions enclosed by shear bands with intersections.

To quantitatively investigate the evolution of shear band orientations and spacing, the orientation angles of shear bands were statistically analyzed. Fig. 2a–c show the histograms of orientation angles. For the deformed sample with a plastic strain of 6%, the orientation angles are mainly centered at around $\varphi = 45^\circ$ (Fig. 2a), which are in agreement with the maximum shear stress direction ($\sim 45^\circ$ from the load axis). With the plastic strain increasing, the orientation angles distribute in a wider range (Fig. 2b and c). For the deformed sample with a plastic strain of 83%, the orientation angles display a multi-peak distribution. The orientation peaks in the distribution histograms can be identified at around $\varphi = -30^\circ$, 0° and 30°, respectively. Interestingly, the absolute values of orientation peaks for the sample with a plastic strain of 83% are not in agreement with the maximum shear stress direction. It implies that the formation and propagation of numerously new fine shear bands are strongly depended on inhomogeneous local stress states. Firstly, with increasing plastic strain, a large amount of uniformly distributed shear band intersections can hinder shear band propagation and further alter their propagating directions [7]. Secondly, shear bands have long range stress field whose magnitude is close to the yield stress of BMG itself [14]. With shear band spacing decreasing, a strongly overlapping internal stress fields form. Then the overlapping internal stress fields can help to trigger the formation of different orientated shear bands. They can also limit shear band propagation and further alter the propagating directions of shear bands. Finally, with the plastic strain increasing, the ratio of height/width for the deformed sample was reduced. In this case, the lateral constraints from friction may increase the complexity of the stress states [15]. Hence, the complex local stress states make the orientations of shear bands deviate the maximum shear stress direction and distribute more widely. In summary, with the plastic strain increasing, the distribution range of orientation angles is more extensive, and the orientation angle distributions gradually exhibit a multi-peak distribution. These features would promote intersecting probability.

In addition, the change of the average shear band spacing with plastic strain was quantitatively analyzed. Fig. 2d shows that the measured average shear band spacing is logarithmically plotted versus plastic strain. As can be seen, the average shear band spacing decreases linearly with plastic strain in log-log plot. It indicates that the average shear band spacing correlates the plastic strain via a power-law relation $d \sim \varepsilon_p^{-\lambda}$ in ductile $Zr_{64.13}Cu_{15.75}Ni_{10.12}Al_{10}$ BMG, where the index $\lambda = 1.22$ ($R^2 = 0.981$). The power-law relation means that shear band spacing can reduce to a very low level in the large deformation stages. This may lead to strong cooperative interactions of multiple shear bands in a short spatial range. Moreover, the index value in the present

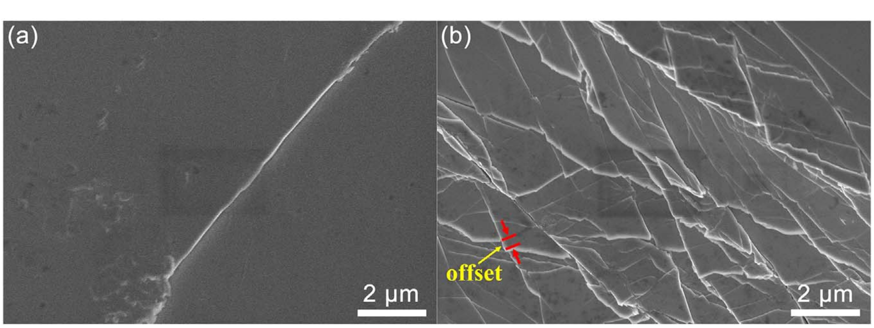

Fig. 1. SEM images of shear bands for the deformed $Zr_{64.13}Cu_{15.75}Ni_{10.12}Al_{10}$ BMG samples with plastic strains of 6% (a) and 83% (b).